Available online at www.sciencedirect.com
SCIENCE DIRECT®
Carbon 43 (2005) 2146–2151
CARBON
www.elsevier.com/locate/carbon

Structure and energetics of carbon nanotube ropes

Zejian Liu [a], Lu-Chang Qin [a,b,*]

[a] Department of Physics and Astronomy, University of North Carolina at Chapel Hill, Chapel Hill, NC 27599-3255, USA
[b] Curriculum in Applied and Materials Sciences, University of North Carolina at Chapel Hill, Chapel Hill, NC 27599-3255, USA

Received 5 November 2004; accepted 24 March 2005
Available online 10 May 2005

Abstract

High-resolution electron microscopy observation and energetic analysis have been performed on ropes formed from single-walled carbon nanotubes. When individual nanotubes are twisted, the nanotube ropes become energetically stable—a configuration that also offers better structural stability. Electron microscopic image simulations of an energetically-stable rope composed of seven single-walled carbon nanotubes have been carried out as well to elaborate the salient features that were observed experimentally.

Keywords: Carbon nanotubes; Electron microscopy; Mechanical properties

1. Introduction

Carbon nanotubes are present mainly in three configurations: single-walled carbon nanotubes [1,2], multi-walled carbon nanotubes [3], and carbon nanotube bundles [4,5]. Engineering and controlling the configurations of carbon nanotubes in the synthesis processes are a crucial step in bringing carbon nanotubes into the envisaged applications [6]. For example, isolated straight single-walled carbon nanotubes are preferred in building molecular electronic circuits [7,8], while carbon nanotube bundles may be favored for pursuing mechanical applications [9]. It has been established and measured that carbon nanotubes have the highest Young's modulus of about 1–2 T Pa [10–13], which offers a great potential for producing high strength components for nanostructured fiber-reinforced composite materials.

Single-walled carbon nanotubes, produced by the popular techniques such as electric arc-discharge [14], laser evaporation [4,5], and chemical vapor deposition [15,16], usually entangle together to form bundles, which can extend up to a total length of millimeters [17]. Raft-like bundles, in which carbon nanotubes are arranged in parallel, are the configuration encountered most often in experiment. Individual carbon nanotubes in the bundles interact with each other through the weak van der Waals forces [18]. However, due to the very fact that the van der Waals forces which hold nanotubes together are weak in the raft-like structure, it is foreseeable that such bundles would not be the ideal configuration of carbon nanotubes for mechanical applications because of the structural weakness. On the other hand, as often encountered in wire ropes, a rope formed from twisted individual strands would not only offer higher load transfer, but also make the configuration structurally much more stable than untwisted raft-like bundles [19,20].

Here we report a study on the structure and energetics of carbon nanotube ropes made from twisted carbon nanotubes by using high-resolution transmission electron microscopy (HRTEM) and numerical simulations.

* Correspondence author. Address: Department of Physics and Astronomy, University of North Carolina at Chapel Hill, Chapel Hill, NC 27599-3255, USA.
E-mail address: lcqin@physics.unc.edu (L.-C. Qin).

0008-6223/$ - see front matter © 2005 Elsevier Ltd. All rights reserved.
doi:10.1016/j.carbon.2005.03.027

Important electron microscopic image features of carbon nanotube ropes were illustrated in a double-strand nanotube rope, a triple-strand nanotube rope and a larger rope, respectively. The energetic stability and formation of these carbon nanotube ropes were analyzed through molecular mechanics calculations. HRTEM image simulations of a septuple-strand carbon nanotube rope were also performed in order to compare with the experimental results.

2. Results and discussion

2.1. Observations of carbon nanotube ropes

The pristine carbon nanotube material produced by electric-arc technique was first dispersed in methanol and agitated in an ultrasonic bath. A small drop of the suspension was then put onto a holey carbon grid and allowed to dry in air. HRTEM imaging of the as-prepared sample was performed in the transmission electron microscope (JEM-2010F equipped with field emission gun) operated at 200 kV and the images were collected on a Gatan ($2k \times 2k$ pixels) CCD camera.

Fig. 1(a) shows an HRTEM image of a double-strand carbon nanotube rope. The two carbon nanotubes of the rope twist with respect to each other along the roping axis by 90° in an axial length of ~18 nm between the left arrow (two dark fringes) and the middle arrow (four dark fringes). The two nanotubes continue to twist about each other by another 90° in the axial length of ~18 nm between the middle arrow and the right arrow. In this configuration the two carbon nanotubes twist about each other along the roping axis at a rate of 5°/nm. The characteristic features in the electron microscope image of the two twisting nanotubes in the rope are indicated by the variation of the dark fringes between the arrows. Fig. 1(b) shows a triple-strand carbon nanotube rope. The three nanotubes in projection on the imaging plane can be clearly observed from the area indicated by the right arrow in Fig. 1(b). By measuring the axial length and the twisting angles, we obtained that the twisting rate for the triple-strand nanotube rope is about 3°/nm, which is smaller than the twisting rate for the plied double-strand nanotube rope shown in Fig. 1(a).

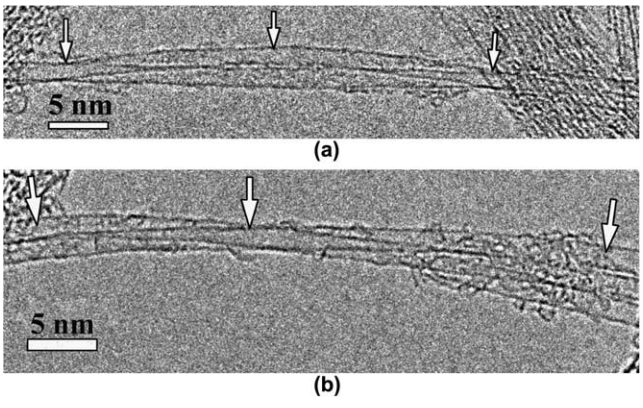

Fig. 1. (a) Transmission electron microscopy image of a double-tubule carbon nanorope. The two tubules twist around their roping axis by about 180° indicated by the three arrows shown in the figure. (b) Transmission electron microscopy image of a triple-tubule carbon nanorope. The areas indicated by the three arrows from left to right show the different projections of the three twisted tubules in the imaging plane.

Twisting of individual nanotubes to form a thicker rope was also observed, although the twisting features are much more complicated than the small nanotube ropes discussed above. Fig. 2(a) shows an HRTEM image of a larger carbon nanotube rope composed of more than 40 individual carbon nanotubes. Letters A, B, and C indicate the areas in which the bundles are imaged along a close-packed row of carbon nanotubes. The images reveal clearly the numbers of nanotube rows seen in projection in the direction of the incident electron beam. The measured distance between A and B is about 67 nm, after which a twist of 60° has been completed, while the distance between B and C is about 42 nm following another twist of 60°. It can be seen that the rate of twisting (~0.9°/nm) between A and B is lower than that (~1.4°/nm) between B and C. However, the image contrast fringes indicated by the white arrows D and E between A and B are very similar to those occurred between B and C, which serve as a fingerprint of plied carbon nanoropes [21]. The magnified areas marked with letters A, B and C showing the number of nanotube rows 7, 6, and 6, are shown in Fig. 1(b)–(d), respectively. In addition, this carbon nanorope is also bent to form an arc with a curvature ~0.02 nm^{-1} with a bending angle about 100°, measured from the angle between the axial directions of the nanotube rope at A and that at C as indicated by the dark arrows.

2.2. Energetic analysis

The structural stability of carbon nanotube ropes was analyzed by carrying out molecular mechanics simulations, which can handle a much larger system of atoms than the ab initio simulations. Bending and twisting of individual carbon nanotubes have already been examined in experiment and simulated by molecular dynamics methods [22–24].

In order to understand the formation and stability of nanoropes observed experimentally, we have investigated the energetics of only straight carbon nanotube ropes with respect to such parameters as the twisting angle and helicity of individual nanotubes. A classical force field method was used to account for the interactions between carbon atoms in the carbon nanotube ropes. To cope with the large model structures

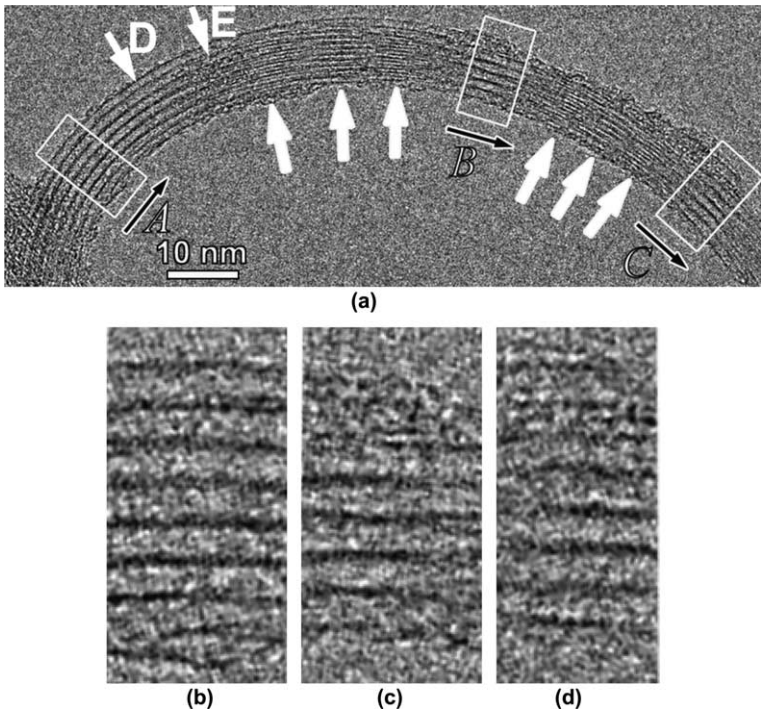

Fig. 2. (a) A twisted carbon nanorope composed of more than 40 individual single-walled carbon nanotubes. The letters A, B, and C indicate the locations where the images reveal the numbers of the nanotube rows in the electron beam direction. The white arrows D and E highlight the salient features of plied carbon nanoropes, whereas the three hollow arrows indicate the roping axis at locations indicated by letters A, B, and C, respectively. Magnified areas indicated by letters A, B, and C are shown in (b), (c) and (d), respectively.

for carbon nanotube ropes that are composed of thousands of atoms, we have only included the diagonal, harmonic terms in the force field [25,26]. The functional forms of the force field can be expressed as follows:

$$E_{\text{tot}} = \sum_b K_2(b-b_0)^2 + \sum_\theta H_2(\theta-\theta_0)^2 + \sum_\phi \times \sum_{j=1}^{3} V_j(1-2\cos(\phi-\phi_j^0)) + \sum_{i>j}\left(\frac{A_{ij}}{r_{ij}^{12}} - \frac{B_{ij}}{r_{ij}^{6}}\right), \quad (1)$$

where $b-b_0$ stands for the bond stretching, $\theta-\theta_0$ stands for the angle bending, the torsion angle ϕ is expressed in the three-term Fourier cosine expansions, K_2, H_2, and V_j are coefficients in the corresponding energy-functional terms, the van der Waals interactions are described by the Lennrad-Jones potential (the final summation terms in Eq. (1)), and no electrostatic interactions were considered in the simulations. The parameters for the Lennard-Jones type interaction potential and all the elastic constants have been derived from the compressibility and the phonon frequencies of graphite [27].

In the implementation of energy minimization for the constructed structure, we used the conjugate gradient method with a convergence of about 4×10^{-3} meV in the overall energy. The energy calculations in the force field applied here are comparable to those calculated by more accurate methods. For instance, twisting an individual nanotube (10, 10) about the tubule axis by 10° in the axial distance of 8.8 nm, the twisting energy increases by ~3 meV/atom, which is in agreement with the results reported by Kwon and Tomanek [28]. In addition, this force field has been also used to study the elastic properties of carbon nanotube bundles [9].

To simplify our simulations but without loss of generality, we first considered a carbon nanotube rope consisting of two strands. The results can be extended to thicker carbon nanotube ropes qualitatively. Fig. 3(a) shows the schematic illustration of a pair of twisting single-walled carbon nanotubes of the same atomic structure (10, 10) (the indices define the perimeter vector on graphene [4]) to form a double-strand rope. Each single-walled carbon nanotube was twisted about its axis by an angle α and then the twisted nanotubes twine around each other to form a nanotube rope of roping angle β. The torsion energy increases harmonically with the distorsion initially and then increases faster as the nanotube is further twisted [28]. From the energetic considerations, due to the increase of strain energy, the distorted structure will not be stable without constraints. However, if the two twisted carbon nanotubes join together, due to the tendency of energy minimization, the structure can be stable energetically while enhancing

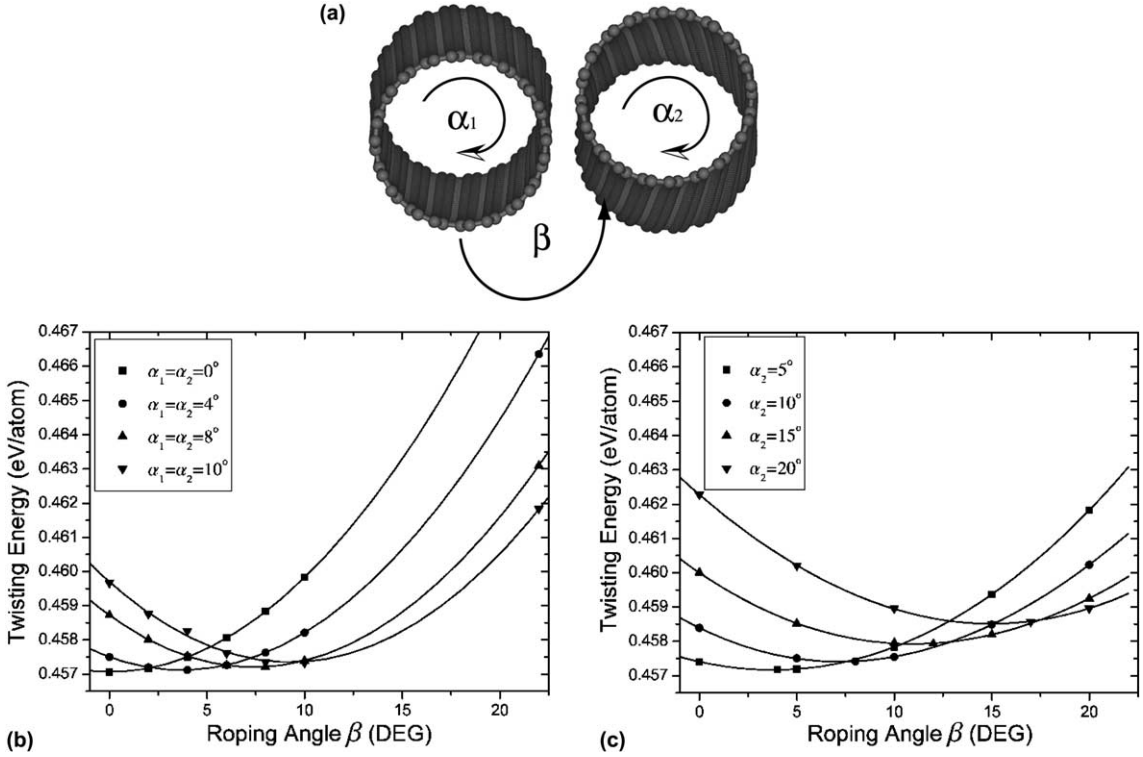

Fig. 3. (a) Schematic of twisting a pair of single-walled carbon nanotubes (10,10) with a length of 8.8 nm to form a carbon nanorope. The two individual tubules are twisted by α_1 and α_2, respectively, and then a plied carbon nanorope is formed with a roping angle β. (b) Relationship between the twisting energy and the roping angle β under the condition of $\alpha_1 = \alpha_2$. α_1 and α_2 were set at the same values of 0, 4°, 8° and 10°, respectively. (c) Relationship between the twisting energy and the roping angle β under the condition of $\alpha_1 \neq \alpha_2$. $\alpha_1 = 0$ and α_2 was set at 5°, 10°, 15°, and 20°, respectively.

structural stability. Fig. 3(b) shows the total formation energy as a function of the twist angle β of the nanotube rope formed by two identical (10,10) nanotubes, each of which is twisted about its own tubule axis by an angle $\alpha = \alpha_1 = \alpha_2$ and then the two twisted nanotubes twine around each other by a roping angle β. From the energetics data shown in Fig. 3(b), we found that, under the condition $\beta \approx \alpha_1 = \alpha_2$, the total strain energy of the twisted nanotube rope has a minimum. Although the total strain energy in the twisting case ($\alpha_1 = \alpha_2 \neq 0$) is still slightly higher than that in the raft-like bundle case ($\alpha_1 = \alpha_2 = 0$), the carbon nanotube rope is still meta-stable, because it would cost energy to get across the energy barrier to recover the parallel configuration. When the twisting angles of the two individual nanotubes are different, i.e., $\alpha_1 \neq \alpha_2$, there exists an optimum roping angle β_0 falling between α_1 and α_2. By assuming that there were no twisting for the first nanotube, i.e., $\alpha_1 = 0$, the optimum roping angle β_0 almost increases linearly with respect to α_2. Fig. 3(c) shows calculated results for the case $\alpha_1 = 0$ and $\alpha_2 = 5°$, 10°, 15°, and 20°, respectively. As in the first case, the plied carbon nanorope is a meta-stable structure when the roping angle β_0 assumes an appropriate value.

On the other hand, since the structure of carbon nanotubes is often helical like the DNA molecule, we have also examined the role of helicity in the formation of a plied carbon nanorope. Fig. 4 shows the relationship between total strain energy and the roping angle of a double-strand carbon nanotube rope in the

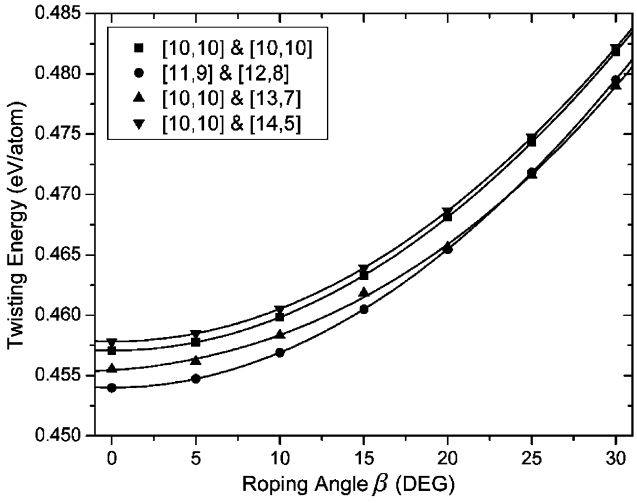

Fig. 4. Twisting energy varies with roping angle for combinations of carbon nanotubes of different helicity—(10,10) and (14,5), (10,10) and (10,10), (11,9) and (12,8) and (10,10) and (13,7). The length of all individual carbon nanotubes is about 8.8 nm.

following combinations: (a) (10,10) and (13,7) ($\Delta\alpha = 9.8°$); (b) (10,10) and (14,5) ($\Delta\alpha = 15.3°$); (c) (11,9) and (12,8) ($\Delta\alpha = 3.3°$); and (d) (10,10) and (10,10) ($\Delta\alpha = 0$), where $\Delta\alpha$ stands for the helicity difference between the two nanotubes. It can be seen from Fig. 3 that the twisting energy has no direct relation with the helicities of the two individual nanotubes as we vary the roping angle of the carbon nanotube rope. This demonstrates that the helicity plays an insignificant role in the formation of a rope-like bundle of carbon nanotubes.

2.3. HRTEM image simulations

In order to understand the contrast of the experimental HRTEM images, imaging contrast simulations were also performed using a model structure. Seven nanotubes of the same structure (10,10) were used to form a septuple-strand carbon nanotube rope, which is shown schematically in Fig. 5(a). The total axial length of the model nanotube rope is 11 nm and it has a twisting rate of 0.9°/nm. Molecular mechanics simulations of the septuple-strand carbon nanotube rope show that the energy variation relative to the roping angle is the same as that for the double-strand nanotube rope. In the HRTEM image simulations, the microscope parameters were chosen in accordance with those for JEM-2010F transmission electron microscope: accelerating voltage $E = 200$ kV, the coefficient of spherical aberration $C_s = 1.0$ mm, diameter of objective aperture 10 nm^{-1}, and the Scherrzer defocus $\Delta f = -50$ nm. Fig. 5(b) shows a simulated HRTEM image along the B direction. The upper white arrow (E) points to the occurrence of finer fringes, which reflect the twisting feature of carbon nanotube ropes as observed experimentally in contrast with the untwisted feature indicated by D.

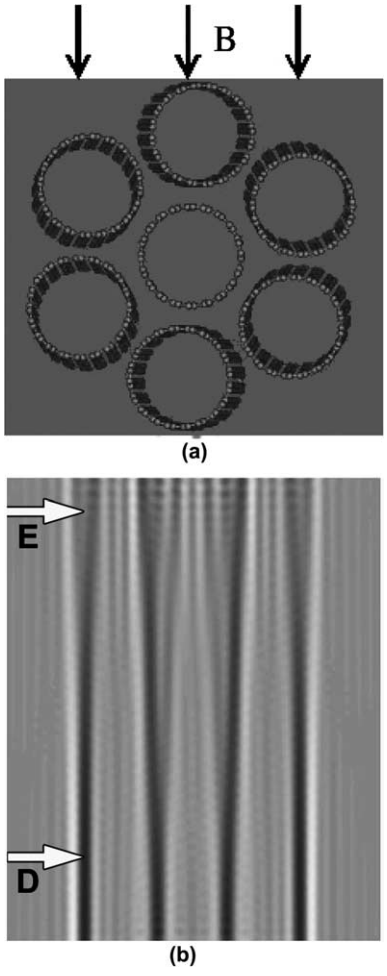

Fig. 5. (a) Cross-sectional view of a model of a rope-like bundle of seven carbon nanotubes with diameter of 11 nm. Six carbon nanotubes twist around the central tubule by approximately 10°, which is comparable to the experimental roping angle of 60° in 70 nm length. (b) Simulated HRTEM image with electron beam incident in the B direction indicated in (a). White arrows D and E highlight the characteristic image features of plied carbon nanoropes.

3. Conclusions

We have observed self-assembled single-walled carbon nanotubes in the form of ropes. A double-strand carbon nanotube rope, a triple-strand carbon nanotube rope and a larger nanorope have been investigated using high-resolution electron microscopy. Molecular mechanics simulations show that, by twisting a single model (10,10) nanotube about its tubule axis, the strain energy increases non-linearly with the twist angle. When two twisted carbon nanotubes join together to form a rope, the nanotube rope is a metastable structure energetically. It has also been demonstrated that the helicity of nanotubes plays an insignificant role in the formation of carbon nanotube ropes. The twisting features observed experimentally in electron micrographs were also explained and simulated using constructed model structures.

Acknowledgment

We wish to thank Professor J.P. Lu and Dr. J. Zhao for helpful discussions.

References

[1] Iijima S, Ichihashi T. Single shell carbon nanotubes of 1-nm diameter. Nature 1993;363(6430):603–5.
[2] Bethune DS, Kiang CH, de Vries MS, Gorman G, Savoy R, et al. Cobalt catalyzed growth of carbon nanotubes with single-atomic-layer walls. Nature 1993;363(6430):605–7.
[3] Iijima S. Helical microtubules of graphitic carbon. Nature 1991;354(6348):56–8.
[4] Thess A, Lee R, Nikolaev P, Dai H, Petit P, et al. Crystalline ropes of metallic carbon nanotubes. Science 1996;273(5274):483–87.

[5] Qin LC, Iijima S. Structure and formation of raft-like bundles of single-walled helical carbon nanotubes produced by laser evaporation. Chem Phys Lett 1997;269(1–2):65–71.
[6] Baughman RH, Zakhidov AA, de Heer WA. Carbon nanotubes—the route toward applications. Science 2002;297:787–92.
[7] Tans SJ, Verschueren RM, Dekker C. Room temperature transistor based on a single carbon nanotube. Nature 1998;393(6680):49–52.
[8] Bezryadin A, Verschueren RM, Tans SJ, Dekker C. Multiprobe transport experiments on individual single-wall carbon nanotubes. Phys Rev Lett 1998;80(18):4036–9.
[9] Lu JP. Elastic properties of carbon nanotubes and nanoropes. Phys Rev Lett 1997;79(7):1297–300.
[10] Calvert P. Materials science-strength in disunity. Nature 1992;357(6377):365–6.
[11] Robertson DH, Brenner DW, Mintmire JW. Energetics of nanoscale graphitic tubules. Phys Rev B 1993;45(21):12592–5.
[12] Overney G, Zhong W, Tomanek DZ. Structural rigidity and low-frequency vibrational-modes of long carbon tubules. Z Phys D 1993;27(1):93–6.
[13] Treacy MMJ, Ebbesen TW, Gibson JM. Exceptionally high Young's modulus observed for individual nanotubes. Nature 1996;381:678–80.
[14] Journet C, Maser WK, Bernier P, Loiseau A, delaChapelle ML, Lefrant S, et al. Large scale production of single-walled carbon nanotubes by electric-arc technique. Nature 1997;388(6644):756–8.
[15] Li WZ, Xie SS, Qian LX, Chang BH, Zou BS, Zhou WY. Large scale synthesis of aligned carbon nanotubes. Science 1996;274(5293):1701–3.
[16] Kong J, Soh H, Cassell A, Quate CF, Dai H. Synthesis of individual single-walled carbon nanotubes on patterned silicon wafers. Nature 1998;395(6705):878–81.
[17] Fanklin N, Dai H. An enhanced CVD approach to extensive nanotube networks with directionality. Adv Mater 2000;12(12):890–4.
[18] Tersoff J, Ruoff RS. Structural properties of a carbon-nanotube crystal. Phys Rev Lett 1994;73(5):676–9.
[19] Costello GA. Theory of wire rope. New York: Springer; 1997.
[20] Qian D, Liu WK, Ruoff RS. Load transfer mechanism in carbon nanotube ropes. Compos Sci Technol 2003;63(11):1561–9.
[21] Qin LC, Iijima S. Twisting of single-walled carbon nanotube bundles. Mater Res Soc Symp Proc 2000;593:33–8.
[22] Despres JF, Daguerre E, Lafdi K. Flexibility of graphene layers in carbon nanotubes. Carbon 1995;33(1):87–9.
[23] Yakobson BI, Brabec CJ, Bernholc J. Nanomechanics of carbon tubes: Instabilities beyond linear response. Phys Rev Lett 1996;76(14):2511–4.
[24] Iijima S, Brabec CJ, Maiti A, Bernholc J. Structural flexibility of carbon nanotubes. J Chem Phys 1996;104(5):2089–92.
[25] Rappe AK, Casewit CJ, Colwell KS, Goddard WA, Skiff WM. UFF a full periodic-table force-field for molecular mechanics and molecular dynamics simulations. J Am Chem Soc 1992;114(25):10024–35.
[26] Rappe AK, Colwell KS, Casewit CJ. Application of a universal force-field to metal complexes. Inorg Chem 1993;32(16):3438–50.
[27] Al-Jishi R, Dresselhaus G. Lattice dynamical model for graphite. Phys Rev B 1982;26(8):4514–22.
[28] Kwon YK, Tomanek D. Orientational melting in carbon nanotube ropes. Phys Rev Lett 2000;84(7):1483–6.